A major purpose of the Technical Information Center is to provide the broadest dissemination possible of information contained in DOE's Research and Development Reports to business, industry, the academic community, and federal, state and local governments.

Although a small portion of this report is not reproducible, it is being made available to expedite the availability of information on the research discussed herein.

LA-UR -87-235

CONF-8610154--2

Received

FEB 03 1987

Los Alamos National Laboratory is operated by the University of California for the United States Department of Energy under contract W-7405-ENG-36

TITLE: EFFECTIVE INTERACTIONS, ELEMENTARY EXCITATIONS, AND TRANSPORT IN THE HELIUM LIQUIDS

LA-UR--87-235

DE87 005097

AUTHOR(S): David Pines, CMS

SUBMITTED TO: "Proceedings of the Banff Conference on Quantum Liquids and Solids," Can. Journ. Physics, 1987.

## DISCLAIMER

This report was prepared as an account of work sponsored by an agency of the United States Government. Neither the United States Government nor any agency thereof, nor any of their employees, makes any warranty, express or implied, or assumes any legal liability or responsibility for the accuracy, completeness, or usefulness of any information, apparatus, product, or process disclosed, or represents that its use would not infringe privately owned rights. Reference herein to any specific commercial product, process, or service by trade name, trademark, manufacturer, or otherwise does not necessarily constitute or imply its endorsement, recommendation, or favoring by the United States Government or any agency thereof. The views and opinions of authors expressed herein do not necessarily state or reflect those of the United States Government or any agency thereof.

By acceptance of this article the publisher recognizes that the U S Government retains a nonexclusive, royalty-free license to publish or reproduce the published form of this contribution or to allow others to do so, for U S Government purposes

The Los Alamos National Laboratory requests that the publisher identify this article as work performed under the auspices of the U S Department of Energy

Los Alamos Los Alamos National Laboratory
Los Alamos, New Mexico 87545

FORM NO 836 R4
ST NO 2629 5/81

DISTRIBUTION OF THIS DOCUMENT IS UNLIMITED

# EFFECTIVE INTERACTIONS, ELEMENTARY EXCITATIONS, AND TRANSPORT IN THE HELIUM LIQUIDS

David Pines, Center for Materials Science
Los Alamos National Laboratory, Los Alamos, NM 87545
and Physics Department*, University of Illinois, Urbana-Champaign
1110 West Green Street, Urbana, IL 61801

To be published in "Proceedings of the Banff Conference on Quantum Liquids and Solids," Can. Journ. Physics, 1987

*Permanent address

## Abstract

Polarization potentials, the self-consistant fields which describe the primary consequences of the strong atom-atom interaction in the helium liquids, are developed for liquid $^4$He and $^3$He. Emphasis is placed on the common physical origin of the effective interactions in all helium liquids, and the hierarchy of physical effects (very short-range atomic correlations, zero point motion, and the Pauli principle) which determine their strength is reviewed. An overview is then given of the application of polarization potential theory to experiment, including the phonon-maxon-roton spectra of $^4$He and $^3$He-$^4$He mixtures, the phonon-maxon spectrum of normal and spin-polarized $^3$He, and the transport properties of superfluid $^4$He and of normal and spin-polarized $^3$He.

## 1. Introduction

In this talk I should like to address the fundamental question of the physical origin and proper description of the effective inderactions between quasiparticles in the helium liquids, that is, in superfluid $^4$He, $^3$He, dilute mixtures of $^3$He in $^4$He, and spin polarized $^3$He. I shall then discuss how these interactions determine the density fluctuation excitation spectra and transport properties of these various liquids, and compare, where possible, theory with experiment. The basic approach I shall be using is polarization potential theory, a minimalist, phenomenological, post-RPA, post-Feynman, post-Landau theory in which physical arguments, constraints from static measurements, sum rules, and continuity arguments are combined to reduce markedly (at times to zero) the parameters required to specify the effective quasiparticle interaction and calculate the elementary excitation spectra. The theory provides a unified and quantitative account of excitations and transport in the helium liquids (1) and has been extended as well to electron liquids (2) and, in work in progress with K. F. Quader and J. Wambach, to nuclear matter.

Polarization potential theory is a unified theory in two senses. First, it enables one to understand the common physical origin of the collective modes in $^3$He and $^4$He in a context in which the remarkable similarity in the restoring forces

responsible for these modes is evident, and in which the physical effects responsible for the differences between quasiparticle interactions in $^4$He and $^3$He at the same density can easily be understood as arising from a combination of zero point motion and the Pauli principle. Second, it provides a systematic basis for calculating the scattering amplitudes for quasiparticle excitations in both $^4$He and $^3$He, and hence yields a natural link between excitation spectra and transport in both systems.

In polarization potential theory, the primary consequences of the strong atom-atom interactions found in the helium liquids are described in terms of self-consistent fields, whose strengths, described by non-local pseudopotentials, determine the effective quasiparticle interactions and the quasiparticle or quasipair masses. It is these fields, the polarization potentials, which provide the wavevector and frequency dependent restoring force responsible for the collective "zero sound" modes which appear as sharp peaks in the density fluctuation excitation spectrum of both liquid $^3$He and $^4$He in the very low temperature limit. In both systems there exists as well an additional mode of excitation, the multiparticle or multipair branch, which is in general comparatively featureless with an average energy which is large compared to the zero sound modes. The coupling between these modes of excitation plays a significant role as well in determining the phonon-maxon-roton spectrum of $^4$He and the

phonon-maxon spectrum of $^3$He; in polarization potential theory it is described by considering the distinct components in the "screened response" of the system to an external field plus the polarization potentials.

My talk is divided into two parts. In the first, mainly didactic part, I discuss at some length the polarization potentials for the various helium liquids. In the second, I give a brief overview of the application of the theory to specific experimental situations, chosen to illustrate how it provides a quantitative account of the density fluctuation excitation spectra and transport properties of superfluid $^4$He, normal $^3$He, spin-polarized $^3$He, and dilute mixtures of $^3$He in $^4$He. In so doing, I shall describe a number of quite recent results, and discuss the close connection between this approach and variational calculations of the phonon-maxon-roton spectrum of liquid $^4$He.

## 2. Effective Interactions: Pseudopotentials and Backflow

There are two key physical effects which must be described in order to obtain a quantitative account of the wavevector and frequency dependent restoring forces responsible for collection behavior in the helium liquids.

- Short-range correlations associated with strong particle interaction, zero-point motion, and, for Fermi systems, the Pauli principle

o Backflow

In polarization potential theory, the short-range correlations are incorporated into the theory by means of a frequency-independent configuration space pseudopotential whose Fourier transform yields a static wavevector dependent restoring force whose strength, in the long wavelength limit, is determined by the system compressibility and (for Fermi systems), the quasiparticle effective mass. Backflow is described as a frequency (and wavevector) dependent restoring force whose strength in the long wavelength limit is determined by the quasiparticle effective mass. Let us consider these effects separately.

A Pseudopotential Description of Effective Interactions

As a particle moves in the liquid it induces density fluctuations which act back on it, as well as on the other particles. These fluctuations, whose mean wave-vector and frequency dependence is described by $\langle\rho(q\omega)\rangle$, give rise to polarization fields which both screen external longitudinal fields and act to provide a restoring force for collective behavior. In polarization potential theory, as in the RPA and Landau Fermi liquid theory, this restoring force is derived from a scalar polarization field,

$$\varphi_{pol}(q,\omega) = f_q^s \langle\rho(q\omega)\rangle; \qquad [1]$$

which couples to the density fluctuations, $\rho_q^+$, by a coupling, $\rho_q^+\varphi_{pol}(q\omega)$. In the RPA, $f_q^s \equiv V_q$, the Fourier-transform of the bare particle interaction; in Landau theory, $f_q^s$ is taken to be momentum-independent, and corresponds to the $\ell = o$ component of Landau's phenomenological interaction between quasiparticles on the Fermi surface. In polarization potential theory, $f_q^s$ is a phenomenological frequency-independent, but momentum-dependent, restoring force, which is calculated by considering the physical behavior of its Fourier transform, a non-local configuration space pseudopotential, $f_s(r)$,

$$f_q^s = \int d^3r\ f^s(r) e^{i\underset{\sim}{q}\cdot\underset{\sim}{r}} . \qquad [2]$$

At low temperatures, $f_o^s$, the spatial average of $f_s(r)$, is known from measurements of the first sound velocity (for $^4$He) or zero sound velocity (for $^3$He). $f^s(r)$ describes an effective interaction between particles in the liquid; how is it related to the bare He atom-atom potential?

The major physical effects which distinguish liquid helium from gaseous helium are at most three-fold:

- o Short-range correlations which enable the helium atoms to avoid, insofar as possible, sampling their mutual very strong short range ($\lesssim 2.7A^{-1}$) repulsive interaction
- o Zero point motion
- o Quantum statistical correlations (eg., the Pauli principle for $^3$He atoms)

Since all three physical effects are predominantly short-range, it follows that at long distances, where liquid correlations are not important, $f^s(r)$ should be identical to the bare atom-atom potential. Aldrich and Pines (3) describe the short range behavior of the pseudopotential $f^s(r)$ with the aid of a simple physical argument, illustrated in Fig. 1, namely that the positional correlations brought about by the strong short-range repulsion between the atoms prevent the atoms from sampling the full consequences of that interaction. Hence, the almost hard-core repulsion of range $\sim 2.68A^{-1}$, found in the bare interaction must go over to a soft-core repulsion, of range $r_c$, which they characterize by an $r^8$ potential of strength a,

$$f^s(r) = a\,(1-r/r_c)^8 \qquad r \lesssim r_c \qquad [3]$$

For a given choice of $r_c$, a simple fitting function is then used to join this part of the potential to the attractive long-range part, taken to be identical to the bare interaction for $r > r_c$.

Because $f_o^s$ is known, for a given choice of $r_c$, a is uniquely determined.

For liquid $^4$He, $f^s(r)$ describes the effective interaction between $^4$He quasiparticles; AP took $r_c$ to be the range of the bare atom-atom repulsive interaction. For liquid $^3$He, $f^s(r)$ is the spin-symmetric average of the effective interaction between parallel and anti-parallel spin quasiparticles,

$$f_3^s(r) = \left[f^{\uparrow\uparrow}(r) + f^{\uparrow\downarrow}(r)\right]/2 \qquad [4]$$

To the extent that the effects of zero point motion and the Pauli principle are small compared to those of the short-range, "hard" core, correlations in determining the $^3$He pseudopotentials, at a given density the shape and range of $f^{\uparrow\uparrow}(r)$ $f^{\uparrow\downarrow}(r)$, and $f^s(r)$ should be quite similar, and one would expect a close relationship between these, and the pseudopotential, u(r), which describes the effective interaction between $^3$He and $^4$He quasiparticles in dilute mixtures of $^3$He in $^4$He. The differences in the pseudopotentials can be characterized by changes in $r_c$, and will arise as a result of zero point motion and the Pauli principle.

For example, the influence of the zero point motion is seen clearly if, at the svp density of $^4$He ($n = 0.0218\ A^{-3}$), one compares $nf_o^s = 27.3K$ with $nu_o = 35.1K$. Replacing a single $^4$He atom by a $^3$He atom gives rise to a spatially averaged $^3$He-$^4$He

particle interaction which is ~30% larger than that between two $^4$He atoms. Hsu and Pines (4), hereafter HP, conclude that the major reason for this increase is an increase in the core radius, the effective range of the repulsive interaction, which both increases slightly the contribution made by the repulsive part of the pseudopotential to its spatial average and reduces substantially the contribution coming from the attractive part. As may be seen in Table 1, with no change in the core height of the pseudopotential, a 2.6% increase in $r_c$ leads to a 30% increase in $f_o^s$. The corresponding values of the spatial averages, core radius, and core height, for the direct part of the effective interactions between $^3$He quasiparticles in liquid $^4$He are likewise given in Table 1. There one sees that for dilute solutions of $^3$He in $^4$He, the Pauli principle acts to increase $V_o^{\uparrow\uparrow}$ by both increasing $r_c^{\uparrow\uparrow}$ over $r_c^{\uparrow\downarrow}$, and by reducing $a^{\uparrow\uparrow}$ compared to $a^{\uparrow\downarrow}$. A comparison of $V_o^{\uparrow\uparrow}$ with $f_o^s$, $u_o$, and $V_o^{\uparrow\downarrow}$ shows that zero point motion plays a much more significant role than the Pauli principle in determining the spatial averages of these pseudopotentials; the enhancement due to zero point motion is some 57%; that due to the Pauli principle is ~5%.

The corresponding parameters for pure $^3$He determined by Bedell, Hess, Hsu, and Pines (in preparation) are also given in Table 1. Note that for pure $^3$He compared with $^4$He at the same density, the spatial average of $f_o^{\uparrow\downarrow}$ is some 70% larger than $f_o^s$,

while the Pauli principle acts to reduce $f_0^{\uparrow\downarrow}$ by some 3%. Bedell et al. find that on going from $^4$He to $^3$He the greater zero point motion of the $^3$He atoms not only leads to an enhanced core radius, but also implies that the correlation-induced screening of the short-range repulsion interaction is somewhat less effective, since $a_{\uparrow\downarrow}$ is increased to 55.7K. The combined effects of the Pauli principle and zero point motion lead to a slightly larger value of $r_c$, and a very slightly reduced value of $a_{\uparrow\uparrow}$, compared to the corresponding values for anti-parallel spin $^3$He quasiparticles. The hierarchy of physical effects on the various restoring forces is thus clearly established: short range potential-induced correlations, which are similar for the various atom-atom interactions, dominate, followed by the influence of zero point motion, with Pauli principle effects coming in a distant third.

The momentum dependent pseudo potentials for the six effective interactions we have considered are shown in Fig. 2. Note that the major differences occur at wavevectors $\lesssim 1A^{-1}$. The increase with q seen at long wavelength is quite a general phenomenon and reflects the changed interplay between the repulsive and attractive parts of the pseudo potentials as one goes to higher moments of $f^s(r)$. Thus if we write

$$f_q^s = f_0^s(1 + q^2 f_2^s + \ldots)$$

then

$$f_0^s = 4\pi \int_0^\infty dr\ r^2 f^s(r) \qquad [5a]$$

$$f_2^s = \frac{-2\pi}{3} \int_0^\infty dr\ r^4 f^s(r)\ . \qquad [5b]$$

In the $r^2$ moment of $f^s(r)$, the short range repulsive part of the pseudopotential wins out over the long range attractive part, but in the $r^4$ moment the situation is reversed. The physical consequence of this behavior is <u>anomalous</u> dispersion, a question to which I shall return shortly.

Finally, the density dependence of the various pseudopotentials is straightforward to obtain. For $^4$He there are no free parameters; $r_c$ is fixed, and only the core height varies with density. Since $f_0^s$ increases with density, the corresponding increase in the core height means that as the density increases the short range correlations in liquid $^4$He are somewhat less effective in reducing the strength of the repulsive part of the interaction. For pure $^3$He, where both the increased zero point motion of the $^3$He atoms and the Pauli principle influence both $r_c$ and $a$, the change of these parameters with density involves some degree of arbitrariness; Bedell et al. choose the density variation of the respective $a$'s, and of $\delta(\equiv r_c^{\uparrow\uparrow} - r_c^{\uparrow\downarrow})$, to be such that the pseudopotentials go over, at svp for pure $^3$He, to those

previously found by Aldrich and Pines to provide the best fit to neutron scattering experiments, while at pressures greater than 21 atm, the results scale with those found for pure $^4$He at similar densities. The resulting parameters are given in Table 2. Note that the influence of the Pauli principle is greatest at svp, and that it becomes weaker as the system density increases.

Backflow

In addition to inducing density fluctuations, as a particle moves in the liquid it induces current fluctuations, which act back on it, thereby changing its effective mass. As Feynman and Cohen first emphasized, these backflow effects are quite important in $^4$He; for a hard sphere moving in a classical liquid the induced current, or backflow, takes a dipolar form, and acts to increase the mass of the sphere by 50%. In polarization potential theory for liquid $^4$He, the induced current fluctuations, $\langle \underset{\sim}{J}(q\omega)\rangle$, are described by a vector field,

$$\underset{\sim}{A}_{pol}(q,\omega) = f_q^v \langle \underset{\sim}{J}(q\omega)\rangle \qquad [6]$$

which couples to the current fluctuations, $\underset{\sim}{j}_q$, by a coupling, $\underset{\sim}{j}_q \cdot \underset{\sim}{A}_{pol}(q\omega)$. Application of particle conservation then leads to the result that the particle effective mass becomes momentum dependent.

$$m_q^* = m + Nf_q^v. \qquad [7]$$

Moreover, since backflow is a purely longitudinal phenomenon, particle conservation links the induced current and density fluctuation according to

$$\langle \underset{\sim}{q} \cdot \underset{\sim}{J}(q\omega)\rangle = \omega \langle \rho(q\omega)\rangle \ . \qquad [8]$$

The resulting effect of backflow is to replace $\varphi_{pol}(q\omega)$, in Eq. (1), by a wavevector and frequency dependent quantity,

$$\varphi_{pol}(q\omega) = \left[f_q^s + (\omega^2/q^2)\ f_q^v\right] \langle \rho(q\omega)\rangle \ . \qquad [9]$$

Absent the effects of zero point motion and the Pauli principle, we would expect the backflow coefficients, $f_q^v$, to be essentially the same in liquid $^3$He and $^4$He at the same density; to the extent that the short-range correlations are mainly responsible for backflow (as they are for $f_0^s$), one can then get $f_0^v$ for $^4$He from the corresponding quantity for $^3$He at the same density, and one would expect a rather similar fall-off of the backflow field strength, $f_q^v$, with increasing momentum transfer. A closer examination of the situation for $^3$He shows that while the effective quasiparticle mass is given by

$$m^* = m + Nf_0^v \equiv m \left[1 + F_1^s \quad 3\right] \qquad [10]$$

where $F_1^s$ is the dimensionless spin-symmetic $\ell = 1$ component of Landau's interaction between quasiparticle on the Fermi surface, the mass defined in Eq. [7] is the momentum-dependent average quasipair effective mass, which characterizes the single quasihole-quasiparticle response to an external field, and may be parametrized by using the Lindhard function for single pair response, with the bare mass m replaced by $m_q^*$. Only in the limit of q = 0 does it equal the quasiparticle mass.

For $^3$He, specific heat experiments tell us what $Nf_0^v$ is as a function of density; AP assumed that at the same density, $Nf_0^v$ would be the same for $^4$He; they determined the q dependence of $m_q^*$ in phenomenological fashion, from their best fit to the phonon-maxon-roton spectrum of $^4$He, and then further assumed that the q dependence of the quasipair mass in $^3$He would be similar. Typical expressions for $Nf_q^v$ for $^4$He are shown in Fig. 3.

It is instructive, and indeed necessary for spin-polarized $^3$He, to separate out the spin-dependence of the backflow terms in $^3$He. To do so, one simply replaces $\underset{\sim}{j}_q \cdot \underset{\sim}{A}_{pol}(q\omega)$ by the expression:

$$\sum_{\alpha\alpha'} j_{q\alpha} h_{\alpha\alpha'}(q) \langle j_{\alpha'}(q\omega)\rangle \ . \qquad [11]$$

in which case we could write:

$$m^*_{q\uparrow} = m + N_\uparrow h_{\uparrow\uparrow}(q) + N_\downarrow h_{\uparrow\downarrow}(q) \qquad [12]$$

with a similar expression for $m^*_{q\downarrow}$. For an unpolarized system, one then has $N_\uparrow = N_\downarrow = N/2$, and $f^v_q = (h_{\uparrow\uparrow} + h_{\uparrow\downarrow})/2$; on the other hand, for a fully spin polarized system, one has $N_\uparrow = N$, and

$$\tilde{m}_\uparrow = m + N\tilde{h}_{\uparrow\uparrow}(q) \qquad [13a]$$

$$\tilde{m}_\downarrow = m + N\tilde{h}_{\uparrow\downarrow}(q) \qquad [13b]$$

so that by using microscopic calculations or physical models, one can proceed to follow the spin polarization dependence of the backflow potentials. Note, further, that for the unpolarized system, $h_{\uparrow\uparrow}(o)$ and $h_{\uparrow\downarrow}(o)$ can be determined directly from a knowledge of $F^s_1$ and the spin-antisymmetric Landau parameter, $F^a_1$. Representative results, which are extremely sensitive to the value of $F^a_1$, at two pressures are given in Table 3. There one sees that the backflow potential for antiparallel spin particles is considerably larger than that for those with parallel spin: the former reflects the combined influence of the short-range, potential-induced correlations and zero point motion, and increases rapidly with density; the latter takes into account the

Pauli principle as well, and is much smaller because the Pauli principle causes particles of parallel spin to spend more time in the attractive region of the effective particle - particle interaction. Indeed, the weak density dependence of the latter suggests that under pressure the particles of parallel spin experience backflow effects which are nearly the same as those applicable at svp; in other words, the Pauli principle prevents particles of parallel spin from sampling the rapid rise in backflow potential brought on by the comparatively ineffective screening.

The influence of the Pauli principle on backflow is even more striking in spin-polarized $^3$He. For the fully polarized system at svp, both microscopic calculations and sum rule arguments yield an up-spin effective mass, $\tilde{m}_\uparrow \cong 0.84m$; thus, at a fixed density the backflow potential, $h_{\uparrow\uparrow}(q)$, <u>decreases</u> with increasing spin polarization, to the point that it vanishes, and then becomes negative in the limit of complete spin polarization, as the Pauli principle causes the up spin quasiparticles to sample more of the attractive interaction between quasiparticles than the repulsive interaction.

## 3. Density-density Response Function

The density fluctuation excitation spectrum is specified by the density-density response function, $R(q,\omega)$ defined as the

linear response of the system to an external field, $\varphi_{ext}(q,\omega)$, coupled to its density fluctuations, $\rho_q^+$. If we consider instead the linear response of the system to the sum of $\varphi_{ext}$ and the polarization potential, $\varphi_{pol}(q,\omega)$, specified by Eq. [9], we obtain

$$\chi^c(q\omega) = \frac{\chi_{sc}(q\omega)}{1-\left[f_q^s + (\omega^2/q^2)\ f_q^v\right]\chi_{sc}(q\omega)} \qquad [14]$$

where $\chi_{sc}(q\omega)$ is the system response to an external potential <u>plus</u> $\varphi_{pol}(q,\omega)$. The poles of $\chi^c(q\omega)$ yield the dispersion relation for the density fluctuation excitation modes; one has therefore

$$1 = \left[f_q^s + (\omega_q^2/q^2)f_q^v\right]\chi_{sc}(q,\omega_q) \qquad [15]$$

where $\omega_q$ is the collective mode excitation energy.

The expression, [14], provides a formal basis for a unified theory of elementary excitations in superfluid $^4$He and normal $^3$He. In it, the role played by frequency and wavevector dependent restoring forces is essentially decoupled from the effects of statistics or temperature; since we have argued that at the same density the corresponding values of $f_q^s$ and $f_q^v$ will be quite similar, the effects of statistics or temperature come in only through $\chi_{sc}(q\omega)$. To the extent that we have described all the consequences of particle interaction by $f_q^s$ and $f_q^v$, then one has $\chi_{sc} = \chi_0^*$, where $\chi_0^*$ is the non-interacting single quasiparticle or

quasipair response: thus for

$$^4\mathrm{He}: \quad \chi_{sc}(q\omega) \cong \chi_o^*(q\omega) = \frac{Nq^2/m_q^*}{\omega^2 - (q^2/2m_q^*)^2} \qquad [16]$$

$$^3\mathrm{He}: \quad \chi_{sc}(q\omega) \cong \chi_L^*(q\omega) \qquad [17]$$

where the expression, [16], represents the excitation of single quasiparticles from the condensate, and $\chi_L^*(q\omega)$ is the Lindhard response function for quasipairs of mass $m_q^*$. To the extent that the collective modes in $^3$He possess a frequency large compared to the single pair energies appearing in $\chi_L^*(q,\omega)$, this expression is well approximated by its high frequency limit, $Nq^2/m_q^* \omega^2$ and the differences in the collective mode energies for $^3$He and $^4$He are determined by their mass difference, and by the influence of zero point motion on $f_q^s$.

The expressions [16] and [17] are, in fact, exact only in the long wavelength limit (where, for example, [15] and [17] yield the usual Landau result); at finite wavevectors, multiparticle excitations begin to play a significant role, and their influence must be taken into account if one hopes to obtain a quantitative account of the excitation spectrum. We consider these now.

## 4. The Two-Branch Spectrum, and Mode-Mode Coupling

Quite generally, for both Bose and Fermi systems, one has two modes of excitation out of the ground state, and hence two branches to the excitation spectrum. For Bose systems, the multiparticle branch corresponds to states characterized by the excitation of two or more quasiparticles from the condensate, [5], while for Fermi systems it corresponds to states in which two or more quasipairs are excited from the filled Fermi sea ground state [6]. The branches can easily be distinguished in the long wavelength limit, since in this limit the frequency of the single quasiparticle or quasipair branch vanishes, while the frequency of the multiparticle or multipair branch is finite. In polarization potential theory, we describe the presence of the two branches by letting $\aleph_{sc}(q\omega)$ contain contributions from both; thus we write

$$\aleph_{sc}(q\omega) = \alpha_q \aleph_o^*(q\omega) + (1 - \alpha_q) \aleph_m(q\omega) \qquad [18]$$

where the strength of the single quasiparticle or quasipair response function contribution to $\aleph_{sc}$ is now measured by vertex renormalization function, $\alpha_q(\leq 1)$, and $\aleph_m(q\omega)$ is the multiparticle or multipair response. Sum rule considerations [5], [6], show that at long wavelengths,

$$\lim_{q\to 0} \alpha_q = 1 - \alpha_2 q^2 + \ldots ; \qquad [19]$$

while to the extent that the characteristic frequencies which enter into $\aleph_m(q\omega)$, $\bar{\omega}_m(q)$, are large compared to those of the collective modes we seek to calculate, we can write:

$$\aleph_m(q,\omega) \cong \aleph_m(q,0) = - \frac{Nq^2/m_q^*}{\langle\omega_m^2(q)\rangle} \qquad [20]$$

For $^4$He, one can obtain $\langle\omega_m^2(q)\rangle$ directly from neutron scattering experiments, while for $^3$He, one can estimate it from Raman scattering experiments. To the extent one knows $\langle\omega_m^2(q)\rangle$ then, the influence of the second, multiparticle or multipair, branch on the collective mode energies is contained in the phenomenological parameter, $\alpha_q$. Since in all cases $\bar{\omega}_m(q) > \omega_q$, the effect of mode-mode coupling will be to depress the collective mode energy, $\omega_q$.

## 5. The Phonon-Maxon-Roton Spectrum of $^4$He

The first major success of polarization potential theory came in its quantitative account of the phonon-maxon-roton spectrum of $^4$He. AP showed that if the momentum dependence of $f_q^v$ was fixed by requiring that $Nf_q^v \sim 1.8m$ in the vicinity of the roton minimum, and $\alpha_q$ and $\aleph_m(q,o)$ were chosen to provide a fit to the excitation spectrum at svp, and were further assumed not to vary with density, then <u>with no free parameters</u> one could get an excellent fit to the measured excitation spectrum for $q \lesssim 2.1\ \text{Å}^{-1}$ at

pressures up to 25 atom. (Recall that $f_q^s$ is fixed by the pressure dependence of the first sound velocity.) A striking verification of the correctness of their pseudopotential was provided by measurements of anomalous dispersion as a function of pressure. At long wavelengths, the phonon dispersion relation takes the form:

$$\lim_{q\to 0} \omega_q = sq\ (1 + \omega_2 q^2 + \omega_3 q^3 + \ldots\ ) \qquad [21]$$

where

$$\omega_2 = \frac{1}{2}\left[f_2^s - \alpha_2 \frac{m^*}{2m} + (4mm_o^* s^2)^{-1}\right] , \qquad [22]$$

$\alpha_2$ is given by Eq. [19] and $\omega_3 = (\pi^2/24 f_o^s) \lim_{q\to 0} \left[f^s(r) r^6\right]$. One sees in Eq. [22] that the positive values of $f_2^s$, characteristic of the AP pseudopotential, bring about anomalous dispersion (a positive value of $\omega_2$) while mode-mode coupling, here represented by $\alpha_2$ (>0), acts to oppose it. As the density increases above its svp value, $f_2^s$ must decrease in a directly calculable way, since the repulsive part of $f^s(r)$ increases [in a fashion fixed by $s(\rho)$], while the attractive part is unchanged; hence, since AP find $\alpha_2(\rho) \cong \alpha_2(\text{svp})$, anomalous dispersion decreases with increasing pressure. Calculation of the wavevector, $q_c$, at which anomalous dispersion ends, requires only a knowledge of $f_q^s$ and $\alpha_q$;

AP found excellent agreement with the direct determination of this quantity (as a function of pressure) by Dynes and Narayanamurthi (7).

In recent work, Coffey and I (manuscript in preparation) have examined anew the polarization potential calculation of the phonon-maxon-roton spectrum. Our reexamination was prompted by two recent developments: Stirling's extraordinarily accurate measurements of the excitation spectrum in the vicinity of the roton minimum (8), and improved microscopic calculations of the excitation spectrum by Manousakis and Pandharipande (9). By making use of the experimentally determined values of $\langle\omega_m^2(q)\rangle$ in Eq. [20], we reduced the number of free phenomonological parameters to one, the multiparticle vertex correction, $\alpha_q$. (Recall that $f_q^s$ is set by the physical arguments presented above, $f_o^v$ by the effective mass in $^3$He at the same density, and $f_q^v$ by its fall-off in the vicinity of the roton minimum.) As shown in Fig. 4, we were able to obtain an excellent account (~0.1% accuracy) of Stirling's experimental results for the roton excitation spectrum, thereby confirming the AP description of a roton as a $^4$He quasiparticle, of effective mass ~$2.8m_o$, moving in a weakly momentum-dependent attractive self-consistent field, $Nf_q^s$, of strength ~-2K, produced by the other quasiparticles.

In our calculations we neglected the dynamic consequences of mode-mode coupling (since we replace $\aleph_m(q,\omega)$ by $\aleph_m(q,o)$ in Eq.

[20]: this approximation should work very well for rotons, and for long wavelength phonons ($q \lesssim 0.5\ A^{-1}$), but for shorter wavelength phonons and maxons, whose energies lie closer to the multiparticle spectrum, it might be expected to be less accurate. A comparison of our results with experiment, given in Fig. 5, shows that this is the case. Also shown in that Figure is the variational calculation of Manousakis and Pandharipande in which the same physical effects (short-range correlations, back-flow, and static mode-mode coupling) are taken into account. For wavevectors up to $\sim 1.3\ A^{-1}$, the two theories give nearly identical results; it may therefore be plausibly argued that the Manousakis/Pandharipande calculations provide a microscopic justification for the polarization potential approach. It is likely that the reason we do considerably better than Manousakis and Pandharipande is that our calculations incorporate a significant reduction in the strength of the backflow potential for $1.5\ A^{-1} \lesssim q \lesssim 2.4\ A^{-1}$.

Finally, as shown in Fig. 6, we see that this modified version of AP theory gives an excellent quantitative account at all pressures of the anomalous phonon dispersion measured in neutron scattering experiments, and of the shift with pressure of the overall spectrum, and of the roton energy and momentum. As I have noted earlier, since $\alpha_q$ is assumed to be independent of density, <u>there are no free parameters in the finite pressure</u>

calculations: the agreement with experiment thus serves to validate the theory.

## 6. Roton-Roton Interactions in $^4$He: Bound States and Transport Properties

Further confirmation of the Aldrich-Pines description of a roton as a $^4$He quasiparticle of mass $\sim 2.8m_0$ came from the work of Bedell, Pines, and Zawadowski, (10) (hereafter BPZ) who argued that the roton-roton interaction could therefore be described in a manner similar to that used for the background $^4$He quasiparticles: that is, by a configuration space pseudopotential, $\tilde{f}(r)$, which at long distances ($\gtrsim r_c$) is identical to the interaction between bare $^4$He atoms, becomes repulsive at $r_c$, and displays a soft-core repulsion for $r \lesssim r_c$ which could be parametrized by an expression of the form, Eq. [3]. At svp, they chose a and $r_c$ so as to yield the experimentally determined binding energy of the $\ell = 2$ bound two-roton state (11) and the roton liquid parameter $f_0$ (analogous to the Fermi liquid parameter, $F_0^s$), which provides a phenomenological description of the shift of the roton energy, $\Delta$, with temperature. At pressures $\gtrsim 5$ bar, they chose these parameters in such a way as to yield the experimental value of the viscosity of $^4$He at $T \gtrsim 1$K. Their results are given in Fig. 8. The physical origin of the larger values of $r_c$ and smaller core heights, a, is likely the zero point motion of the rotons; their

variation under pressure resembles that found for the $^3$He pseudopotentials.

BPZ used their pseudopotential to calculate the roton-roton scattering amplitude which determines the existence of bound states and the transport properties of $^4$He at $T \gtrsim 1K$. Because of the substantial structure in the Fourier transform of their pseudopotential (cf Fig. 8), they found that while substantial binding could exist in partial wave channels with $\ell \gtrsim 4$, for $P \gtrsim 5$ bar, no $\ell = 2$ bound state would exist. This prediction of their theory has been verified in the experiments of Ohbayashi and his collaborators, which have been reported on at this meeting. (12) Further confirmation of the correctness of their pseudopotential came from the good agreement they found between theory and experiment for the roton lifetime as a function of temperature, and for the roton liquid parameter, $f_1$, (analogous to the Landau $F_1^s$, which determines the roton liquid corrections to the normal fluid density).

## 7. The Phonon-Maxon Spectrum of Liquid $^3$He

Perhaps the most striking confirmation of the AP theory of the density fluctuation collective modes in $^3$He came from their quantitative prediction of a well-defined phonon-maxon spectrum for $q \lesssim 1.4\ \text{Å}^{-1}$. On the basis of the failure by Scherm et al (13), in their pioneering experiment at L.L.L., to see a

well-defined zero sound mode for $q \gtrsim 1.4\ A^{-1}$. AP concluded that the value of the repulsive core radius for $^3$He at svp, $r_c$, was ~3.1 A, this led them to the spectrum, shown in Fig. 10, which was damped by single quasipair excitations for $q \gtrsim 1.4\ A^{-1}$. The subsequent elegant neutron scattering experiments, carried out by Skold and his collaborators at Argonne (14), gave a phonon-maxon spectrum in close agreement with the AP prediction, in that not only did Skold et al find that for $q \lesssim 0.8\ A^{-1}$, the zero sound portion of the spectrum exhibited the substantial anomalous dispersion calculated by AP, but that for $0.8\ A^{-1} \lesssim q \lesssim 1.4\ A^{-1}$ the spectrum was quite flat, with a maxon energy ~13K, close to the value ~12K predicted by AP.

It should be emphasized that the entire excitation spectrum discovered by Skold et al is in a non-Landau regime, in that the wavevectors under study are $\gtrsim p_f$ and the energies under investigation are large compared to $E_F$. As I first showed in 1965 (15), well-defined density fluctuation excitations in a non-Landau regime are just what one would expect from a strongly coupled neutral quantum liquid such as $^3$He, for the same reason that the zero sound modes in liquid $^4$He exist above the λ-point; in both $^3$He and $^4$He the strength of the self consistent field responsible for the collective mode is sufficiently large that Landau damping (for $^4$He) and multiparticle damping (for $^4$He) only occur at considerably elevated values of wavevectors and temperatures

Because these collective modes possess energies large compared to the characteristic single particle or pair energies, they resemble closely the plasmons of charged particle systems, in that the energy of the collective mode depends only weakly on temperature (Sköld and Pelizzari (14) found almost no change in the density fluctuation spectrum of $^3$He on going from 40 mK, a "good" Landau-regime temperature, to 1200 mK, a thoroughly "non-Landau regime" temperature) and on whether the system is in a normal or superfluid state.

Let me now turn briefly to the changes one would anticipate in the density fluctuation excitation spectrum with pressures; the experimental situation will be summarized by Reinhard Scherm (16) in a later talk at this conference. Three aspects are immediately clear: first, the initial slope of the $\omega_q$ curve, which is identical to the zero sound velocity, $s_0$, will increase; second, since sum rule arguments tell us that at long wavelengths the strength of the zero sound mode is given by $Z_q \equiv hq/2ms_0$, quite generally we would expect the strength of the collective mode to decrease with increasing pressure; third, since the quasiparticle effective mass increases with pressure, single quasipair excitations will play an even less important role at pressure than they do at svp (where their role is negligible for $q \lesssim 1\ \text{Å}^{-1}$). Thus anomalous dispersion, maxon energies, and damping, will

depend only on an interplay between the changes in the non-local restoring force, $f_q^s$, and the multipair spectrum, with pressure.

If, for example, neither the effective range of the repulsive part of $f^s(r)$ nor the multipair spectrum change with increasing pressure, one would have a situation directly analogous to that we have considered earlier for $^4$He: anomalous dispersion would decrease. On the other hand, if both $r_c^{\uparrow\downarrow}$ and $r_c^{\uparrow\uparrow}$ decrease with pressure, as the fit to transport properties obtained by Bedell et al suggests they will, while the multipair spectrum remains unaffected by pressure, then calculations with Hess carried out subsequent to this meeting show that initially one will get an increase in the magnitude and extent of anomalous dispersion with pressure, since the reductions in $r_c$, which enhance the contribution made by the attractive part of the potential to the various moments of $f_s(r)$, outweigh, in the $r^4$ moment, the enhancement in the repulsive contribution coming from the increase in the core height, a. Finally, if, as the preliminary analysis (16) of their experiments by Scherm et al shows, the damping of the zero sound mode increases with pressure, while anomalous dispersion does not show a corresponding increase, this furnishes an unambiguous signal that the strength of the low frequency tail of the multipair spectrum must increase with pressure (the failure to observe an increase in anomalous dispersion rules out the alternative explanation, that the damping is due to the decay of a

zero sound mode into two lower energy modes). Under these circumstances, the key physical quantities (the density dependence of anomalous dispersion, the onset of the maxon regime, the magnitude of the maxon energy, and maxon damping) will depend on the details of the interplay between the changes in $f_q^s$ and the multipair spectrum. That the strength of the low energy part of the multipair spectrum should increase with pressure is, in fact, not too surprising, since one might expect that this portion of the multipair spectrum would be sensitive to changes in the quasiparticle Fermi energy, with a decrease in the Fermi energy implying a corresponding increase in the low energy multipair strength.

## 8. Dilute Solutions of $^3$He in Superfluid $^4$He

The density fluctuation excitation spectrum of $^3$He - $^4$He mixtures provides information on the extent to which the presence of the $^3$He atoms modifies the phonon-maxon-roton spectrum of the background $^4$He liquid, and on the quasiparticle and density fluctuation spectra of the $^3$He atoms. Neutron scattering provides a direct probe of these spectra, while indirect information on the $^3$He quasiparticle spectrum is provided by specific-heat and second-sound experiments.

Aldrich, Hsu, and Pines (17) have shown that the rather complex wavevector and concentration-dependent shifts in the

phonon-maxon-roton spectrum found experimentally by Hilton, Scherm, and Stirling (18) at $T \lesssim 0.75K$, and shown in Fig. 11, find a quantitative explanation as the superposition of two distinct physical effects:

i. The introduction of $^3He$ atoms into liquid $^4He$ reduces the system density, and so changes the liquid $^4He$ restoring forces responsible for the $^4He$ collective mode spectrum. This effect is the largest numerically.

ii. A direct interaction (mode-mode coupling) between the phonon-maxon-roton branch and the $^3He$ density fluctuation excitation branch of the overall spectrum. The resulting shift is sensitive to the concentration-dependent mode-mode coupling constant and to the temperature-dependent response function for the $^3He$ quasiparticle; it thus depends on $^3He$ concentration, on temperature, and on the exact form assumed for the $^3He$ quasiparticle spectrum.

The density-change shift provides a test of the Aldrich-Pines $^4He$ pseudopotentials at lower (than svp) $^4He$ densities, while the mode-mode coupling shift provides a test of the concentration and momentum dependence of the Hsu-Pines $^3He$-$^4He$ pseudopotentials, and of the $^3He$ quasiparticle spectrum. The excellent agreement between theory and experiment for the sum of these two shifts provides strong evidence for the correctness of the concentration

and momentum dependence of both the Aldrich-Pines $^4$He pseudopotentials and the Hsu-Pines $^3$He-$^4$He pseudopotentials, as well as for the $^3$He quasiparticle spectrum derived by Greywall (19) from specific heat and second sound experiments, since only with the latter does one obtain good agreement with the neutron scattering experiments.

Aldrich et al (17) also show that for $^4$He excitations in the vicinity of the roton momentum, and temperatures $\gtrsim$ 1K, the scattering of rotons against thermally excited $^3$He quasiparticles produces a significant shift in energy; the effect is proportional to the $^3$He concentration, while its variation with temperature is governed by the $^3$He quasiparticle spectrum. As may be seen in Fig. 12, on taking this effect into account with the Greywall spectrum they find excellent agreement with experiment for the temperature dependence of the total energy shift. Finally, they find that with the Greywall spectrum they are able to obtain good agreement between theory and experiment for the peaks of the $^3$He density fluctuation excitation spectrum.

## 9. Transport Properties of $^3$He

The four measurable transport properties of normal $^3$He, the thermal conductivity, viscosity, spin diffusion, and quasiparticle lifetime, depend upon various angular averages of the squared singlet and triplet quasiparticle - quasiparticle scattering

ampliudes (QSA's). Following the pioneering QSA calculation of Dy and Pethick (20), the s-p approximation, QSA's have been determined during the past decade in a number of different ways:

i. using potential-scattering models, involving two phenomenological local potentials, chosen to yield both Landau parameters and the best fits to transport properties (21) (paramagnon models (22) represent a special class of such models).

ii. by using a Bethe-Salpeter equation to relate QSA's to the AP polarization potentials, which represent effective quasiparticle-quasihole interactions.

iii. by separating the quasiparticle interaction into two pieces, one direct, one induced, and then using a phenomenological approach combined with either sum rule arguments or approximate microscopic calculations to specify the direct interaction, while obtaining the induced interactions by symmetry arguments (23) (24).

For each of these approaches the calculated transport properties are in quite good ($\lesssim$ 10%) agreement with experiment. Deciding on their respective merits is therefore, at least in part, a matter of taste.

The virtue of the third approach, which is a generalization of the induced-interaction model of Baym and Brown (25) is that once the input potentials are fixed at a given density (say svp),

one is able to get correctly the density dependence of both the Fermi liquid parameters and the transport properties. The recent calculations based on this approach by Ainsworth and Bedell (23), and by Pfitzner and Wolfle (24), differ in detail, but are essentially similar, and prove equally successful in relating to experiment. Both sets of calculations yield q-dependent polarization potentials, which however, differ considerably from the AP results, consequently if these induced-interaction potentials are used to calculate the density fluctuation excitation spectrum, the agreement with experiment is not good.

The second approach, first developed by Bedell and Pines (26), uses the previously determined AP polarization potentials as input to a generalized Bethe-Salpeter equation for the QSA's. A simple algorithm was then used to guarantee the exchange symmetry of the resulting scattering amplitudes. These scattering amplitudes were not however, self-consistent, in that when substituted into a Bethe-Salpeter equation for the quasiparticle-quasihole scattering amplitudes, the AP polarization potentials were not recovered. This deficiency was subsequently remedied by Pfitzner and Wolfle (27) whose fully self-consistent QSA's led to a modest change in the transport coefficients.

In their calculations, BP took $\delta(= f_c^{\uparrow\uparrow} - f_c^{\uparrow\downarrow})$ to be a free parameter, and selected that value which gave the best fit to the transport experiments. While $\delta$ is small (varying from 0.11 at sup

to ~0.007 at $P \gtrsim 20$ atm), it plays an important role in determining $f_q^a$, which in turn plays a significant role in determining transport properties. Since neutron scattering experiments are not at present capable of resolving $\delta$ to this degree of accuracy, it is only by combining transport calculations with neutron scattering results that one finally arrives at a conplete specification of both $f^{\uparrow\uparrow}(r)$ and $f^{\uparrow\downarrow}(r)$. For a further discussion of these and related matters, the interested reader is referred to a forthcoming paper (Bedell, Hess, Hsu, and Pines, in preparation).

In concluding this discussion, let me emphasize that any complete and unified theory of $^3$He should be able to give a quantitative account of both the polarization potentials (i.e. q-dependent Landau parameters) and the QSA's. So far it would seem that the polarization potential approach does this best, since it describes accurately both the density and spin fluctuation excitation spectra, and yields, given the simplicity of the BP ansatz, an amazingly accurate QSA, one which Ainsworth and Bedell (23) have shown is quite close to that calculated using the induced interaction model. The next significant improvement will likely come from solutions of the parquet equations for the coupled scattering amplitudes, since only in this way is one likely to obtain a microscopic theory for both the polarization potentials and the QSA's.

## 10. Fully Spin-Polarized $^3$He

Hess, Pines, and Quader (in preparation) have studied effective interactions, elementary excitations, and transport in $^3\tilde{\mathrm{He}}$, spin-polarized $^3$He in the fully polarized limit, and I should like to comment briefly on their results. In constructing the polarization potential, $\tilde{f}^{\uparrow\uparrow}(r)$, in this limit, they make use of a simple ansatz for its spatial average, $\tilde{f}_o^{\uparrow\uparrow}$, namely that at a given density the upper limit to the physical effect of spin polarization on $f_o^{\uparrow\uparrow}$ is given by the magnitude of Pauli principle changes on going from $f_o^{\uparrow\downarrow}$ to $f_o^{\uparrow\uparrow}$ for the unpolarized system. Thus

$$\tilde{f}_o^{\uparrow\uparrow} - f_o^{\uparrow\uparrow} \lesssim f_o^{\uparrow\uparrow} - f_o^{\uparrow\downarrow} \equiv 2f_o^a \qquad [23]$$

(Recall that Pauli principle effects are small compared to those of short-range potential induced correlations or zero point motion, and are typically $\sim 2NF_o^a \sim 2K$.) By combining this ansatz with the forward scattering rum rule, and on assuming that only the $\ell = 0$ and $\ell = 1$ moments play a role in determining quasiparticle interaction at the Fermi surface, they obtain values for $m^*/m$ and the compressibility which are close to the microscopic calculations of Manousakis et al (28).

The resulting density fluctuation excitation spectrum depends on the assumed form of the wavevector dependence of the backflow potential. HPQ consider two limits; one in which the effects of

spin polarization on $m_q^*$ is assumed to be wavevector independent; one in which this effect is assumed to operate predominantly at long wavelengths, so that by the time one reaches, say, $q \sim 1.8\ \text{Å}^{-1}$, there would be little difference between $\tilde{m}_q^*$ and $m_q^*$. In the first case the reduction of $\tilde{m}_q^*$ leads to a substantial qualitative change in the spectrum: the onset of Landau damping is much earlier, and no maxon regime is found. In the second, the spectrum is qualitatively the same; the wavevector which characterizes the onset of Landau damping is only slightly reduced.

HPQ construct the $^3\tilde{\text{He}}$ QSA's from $\tilde{f}_q^s$ and $\tilde{m}_q^*$ following an approach similar to that which BP used for $^3$He, and use these to calculate the thermal conductivity and viscosity. Their results are qualitatively similar but quantitatively different from these calculated by Bedell and Quader (29) using the s-p approximation; both transport coefficients are some two orders of magnitude larger than the corresponding quantity for unpolarized $^3$He. Transport in spin-polarized $^3$He may thus be expected to vary rapidly with spin polarization; indeed, Hess and Quader (30) find for the partially polarized liquid that the viscosity initially decreases with spin polarization, a decrease which agrees well with the recent measurements of Archie (31) before starting, at ~30% polarization, a dramatic increase.

## 11. Concluding Remarks

I hope that this review of the physical origin of polarization potentials in the helium liquids has served to bring out their common physical origin, and that the brief overview of the application of the theory to experiment provides evidence of its success in making possible a unified and quantitative theory of excitation and transport in these systems. There was not time in either the talk, or in this written account, to review all the applications of the theory or consider in more detail its relation to variational nd microscopic theories. Thus I have not described the way in which it makes possible a derivation of the momentum dependence of the over-all interaction between $^3$He quasiparticles in dilute mixtures of $^3$He in $^4$He, nor compared theory with experiment for the transport properties of these mixtures (4), or discussed quasiparticle interactions in partially spin-polarized $^3$He. To cite two further examples: the close relationship between the results of polarization potential theory and variational calculations of the phonon-maxon-roton spectrum of $^4$He is highly suggestive, and deserves further exploration, while the connections between polarization potential theory and the recent "Gutzwiller" calculation of effective interactions in $^3$He by Anderson, Vollhardt, and Wölfle (preprint) likewise deserve further study.

## 8. Acknowledgments

I should like to take this opportunity to thank my collaborators in this research, C. H. Aldrich, K. Bedell, D. Coffey, D. Hess, W. Hsu, C. J. Pethick, K. F. Quader, and A. Zawadowski for helpful and stimulating discussions, to thank the Center for Materials Science (Los Alamos) for its warm hospitality and support during the preparation of this manuscript, and to acknowledge the support of the National Science Foundation (NSF Grant DMR 85-21041).

Table 1. Comparison of the spatial average, core radius, and core height of the pseudopotentials which describe effective interactions between quasiparticles in helium liquids at a density of 0.0218 $A^{-3}$ (svp for $^4He$) (from Hsu and Pines).

| System | Interaction | Spatial Average (K) | Core Radius (A) | Core Height (K) |
|---|---|---|---|---|
| $^4He$ | $^4He$-$^4He$ | $f_o^s = 27.3$ | 2.68 | 49.3 |
| $^4He$ | $^3He$-$^4He$ | $u_o = 35.1$ | 2.751 | 49.3 |
| $^4He$ | $^3He^\uparrow$-$^3He^\downarrow$ | $V_o^{\uparrow\downarrow} = 42.8$ | 2.821 | 49.3 |
| $^4He$ | $^3He^\uparrow$-$^3He^\uparrow$ | $V_o^{\uparrow\uparrow} = 45.0$ | 2.993 | 39.8 |
| $^3He$ | $^3He^\uparrow$-$^3He^\downarrow$ | $f_o^{\uparrow\downarrow} = 46.5$ | 2.773 | 55.7 |
| $^3He$ | $^3He^\uparrow$-$^3He^\uparrow$ | $f_o^{\uparrow\uparrow} = 45.2$ | 2.780 | 54.2 |

Table 2. A comparison, at various densities, of the spatial average, core radius, and core height of the pseudo potentials which describe the effective interactions between quasiparticles responsible for the restoring forces for zero sound and spin density fluctuation excitations in $^3$He.

| Pressure (bar) | $f_o^{\uparrow\downarrow}$ (K) | $f_o^{\uparrow\uparrow}$ (K) | $r_c^{\uparrow\downarrow}$ | $r_c^{\uparrow\uparrow}$ | $a^{\uparrow\downarrow}$ | $a^{\uparrow\uparrow}$ |
|---|---|---|---|---|---|---|
| svp | 11.8 | 10.1 | 3..0 | 3.03 | 23.2 | 20.9 |
| 5 | 22.4 | 20.8 | 2.936 | 2.953 | 32.0 | 30.1 |
| 10 | 31.0 | 29.6 | 2.878 | 2.890 | 39.9 | 38.2 |
| 15 | 38.7 | 37.3 | 2.826 | 2.833 | 47.4 | 45.9 |
| 21 | 46.5 | 45.2 | 2.773 | 2.780 | 55.7 | 54.2 |
| 34.36 | 58.8 | 57.6 | 2.705 | 2.712 | 68.8 | 67.2 |

Table 3. Spin-dependent backflow potential parameters for unpolarized $^3$He.

| P (bar) | $F_1^a$ | $F_1^s$ | $Nh_{\uparrow\uparrow}/m$ | $Nh_{\uparrow\downarrow}/m$ |
|---|---|---|---|---|
| svp | -0.5 | 5.3 | 1.2 | 2.3 |
| 27 | -1.0 | 12.5 | 1.6 | 6.8 |

Legends for Illustrations

Figure 1. Schematic drawing of liquid helium pseudopotentials: a) configuration space, . . . bare interaction, _____ pseudopotential; b) momentum space.

Figure 2. Momentum dependent pseudopotentials which describe the effective interaction between He atoms in very dilute ($x \to o$) mixtures of $^3$He in $^4$He, compared with the corresponding potentials for pure $^3$He at the same density [from Ref. (4)].

Figure 3. Backflow potentials in liquid $^4$He as a function of pressure [from Ref. (3)].

Figure 4. Comparison of the calculated excitation spectrum in the vicinity of the roton minimum with experiment [8].

Figure 5. Comparison with experiment of the polarization potential and variational [(Ref. 9), shown by triangles] results for the phonon-maxon-roton excitation spectrum; in both theoretical calculations, dynamic mode-mode coupling corrections are neglected.

Figure 6. Comparison at five pressures of the calculated anomalous phonon dispersion with neutron scattering measurements [Aldrich, Coffey, and Pines, in preparation].

Figure 7. The pressure dependence of the phonon-maxon-roton spectrum of $^4$He.

Figure 8. The configuration space pseudopotential which describes roton-roton interactions, calculated at two pressures, and compared with that which describes the interaction between background $^4$He quasiparticles.

Figure 9. The momentum-dependent roton-roton pseudopotential at two pressures.

Figure 10. Comparison between theory and experiment for the collective modes and mean single pair energies in the density fluctuation spectrum of liquid $^3$He. The dot-dashed line represents the phonon-maxon spectrum predicted by Aldrich and Pines in advance of its observation by Skold et al [14], while the solid line is the subsequent Aldrich-Pines calculation in which a 3% lower value of $r_c$ was used [3]. The dashed line is the AP calculation of the mean quasipair excitation energy, which depends sensitively on the quasipair mass, $m_q^*$, and which is seen to agree with experiment for $q \gtrsim 1.5\ \text{Å}^{-1}$.

Figure 11. Energy shifts of the phonon-maxon-roton spectrum in dilute mixtures of $^3$He in $^4$He, measured at T = 0.75K by Hilton et al [Ref. (16)] as a function of concentration, x.

Figure 12. Comparison of theory and experiment for the temperature-dependent energy shift of the phonon-maxon roton spectrum in a 6% solution of $^3$He in $^4$He [from Ref. (17)].

List of References


1. D. Pines, in Highlights of Condensed Matter Theory, Course 89 of the Varenna Summer School, Soc. Italiana di Fisica, Bologna, Italy, pp. 580-643, 1985.
2. N. Iwamoto and D. Pines, Phys. Rev. B 29, 3924 (1984).
3. C. H. Aldrich and D. Pines, J. Low Temp. Phys. 25, 677 (1976); ibid v. 32, 689 (1978); C. H. Aldrich, C. J. Pethick, and D. Pines, J. Low Temp. Phys. 25, 691 (1976); Phys. Rev. Lett. 37, 845 (1976).
4. W. Hsu and D. Pines, J. Stat. Phys. 38, 273 (1985).
5. A. Miller, D. Pines, and P. Nozieres, Phys. Rev. 127, 1452 (1962).
6. D. Pines and P. Nozieres, Theory of Quantum Liquids, Vol. 1. (W. A. Benjamin, N.Y. 1966).
7. R. C. Dynes and V. Naravanamurthi, Phys. Rev. B 12, 1720 (1975).
8. W. G. Stirling, Proc. Second Intl. Conf. on Phonon Physics, ed. J. Kollar, N. Kroo, N. Menyhard, and T. Siklos (World Scientific, Singapore, 1985).
9. E. Manousakis and V. R. Pandharipande, Phys. Rev. B 30, 5062 (1984).
10. K. S. Bedell, D. Pines, and A. Zawadowski, Phys. Rev. B 29, 102 (1984).
11. T. J. Greytak, in Quantum Liquids, ed. J. Ruvalds and T. Regge, North-Holland, Amsterdam, 1968) p. 21.
12. K. Ohbayashi, Proc. this conference.
13. R. Scherm, W. G. Stirling, A.D.B. Woods, R. A. Cowley, and G. J. Coombs, J. Phys. C., 7, 1341 (1974).
14. K. Sköld, C. A. Pelizzari, R. Kleb, and C. E Ostrowski, Phys. Rev. Lett. 37, 842 (1976); K. Sköld and C. A. Pelizzari, J. Phys. C. 11, L589 (1978).
15. D. Pines, in Quantum Fluids, ed. D. Brewer (North-Holland, Amsterdam, 1966), p. 257.
16. R. Scherm, Proc. this conference.
17. W. Hsu, D. Pines, and C. H. Aldrich, Phys. Rev. B 32, 7179 (1985).
18. P. A. Hilton, R. Scherm, and W. G. Stirling, J. Low Temp. Phys. 27, 851 (1977).
19. D. S. Greywall, Phys. Rev. Lett. 41, 177 (1978); Phys. Rev. B 20, 2643 (1979).
20. K. S. Dy and C. J. Pethick, Phys. Rev. 185, 373 (1969).
21. J. A. Sauls and J. W. Serene, Phys. Rev. B 24, 183 (1981).
22. K. Levin and O. Valls, Phys. Rev. B 20, 105; ibid, 120 (1979).

23. T. Ainsworth and K. S. Bedell, Phys. Rev. B. (in the press) (1987).
24. M. Pfitzner and P. Wölfle, Phys. Rev. B (in the press) (1987).
25. S. Babu and G. E. Brown, Ann. Phys. 78, 1 (1973).
26. K. S. Bedell and D. Pines, Phys. Rev. Lett. 45, 39 (1980).
27. M. Pfitzner and P. Wölfle, J. Low Temp. Phys. 51, 535 (1983).
28. E. Manousakis, S. Fantoni, V. R. Pandharipande, and Q. N. Usmani, Phys. Rev. B 28, 3770 (1983).
29. K. S. Bedell and K. F. Quader, Phys. Lett. 96A, 91 (1983).
30. D. Hess and K. F. Quader, Proc. this conference, and Phys. Rev. Lett. (to be published), 1987.
31. C. Archie, Proc. this conference.

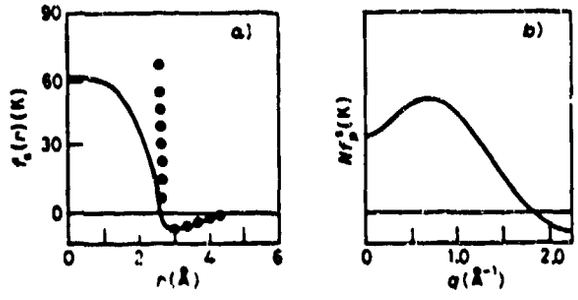


Fig. 1. – Schematic drawing of liquid-helium pseudopotentials: *a*) configuration space, ••• bare interaction, ——— pseudopotential; *b*, momentum space.

Figure 1

- Place (b) below (a)
- Blow up both to standard size specified in instructions

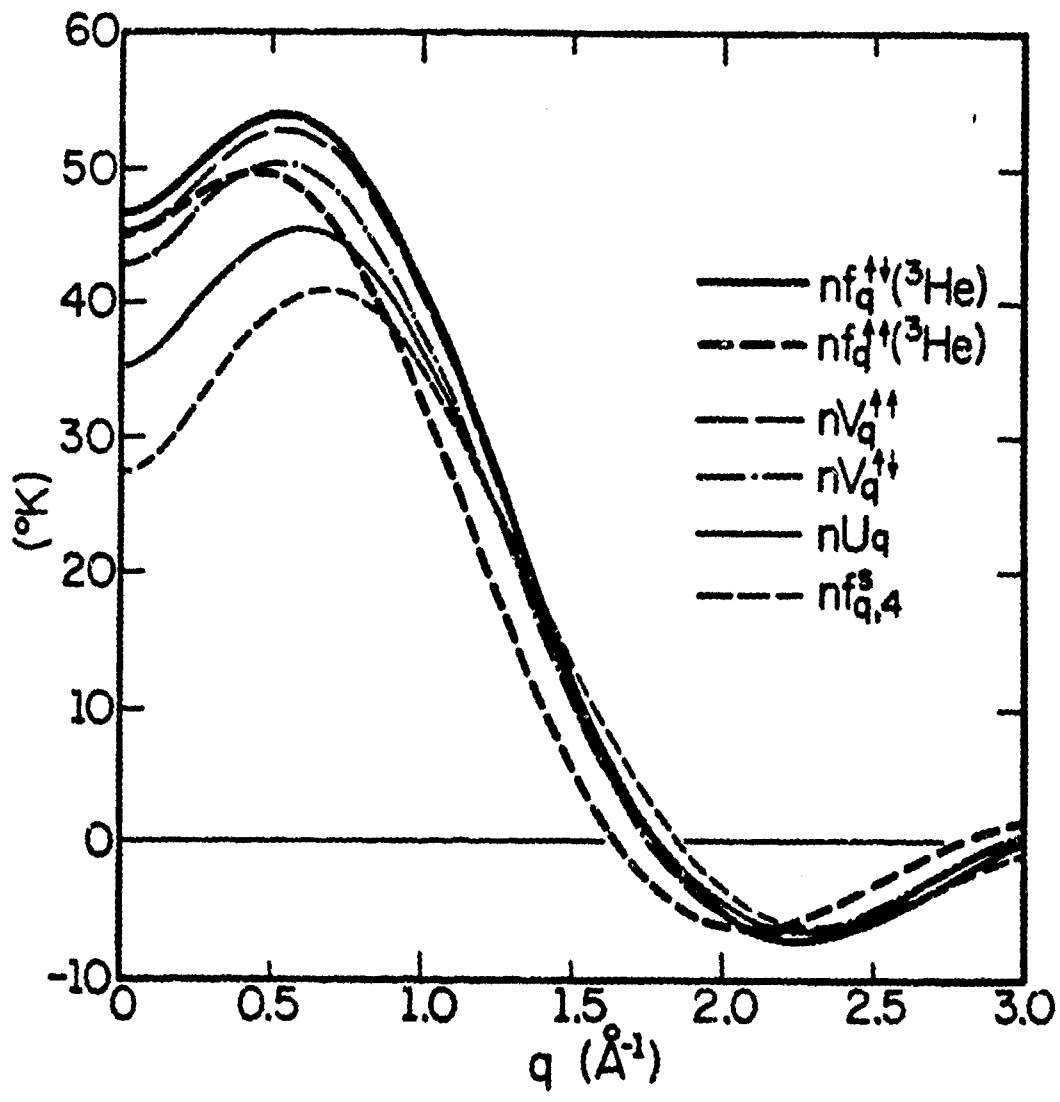
60
50
40
30
20
10
0
-10
(°K)
0
0.5
1.0
1.5
2.0
2.5
3.0
q (Å⁻¹)
$nf_q^{\uparrow\downarrow}(^3He)$
$nf_q^{\uparrow\uparrow}(^3He)$
$nV_q^{\uparrow\uparrow}$
$nV_q^{\uparrow\downarrow}$
$nU_q$
$nf_{q,4}^{s}$

Figure 2

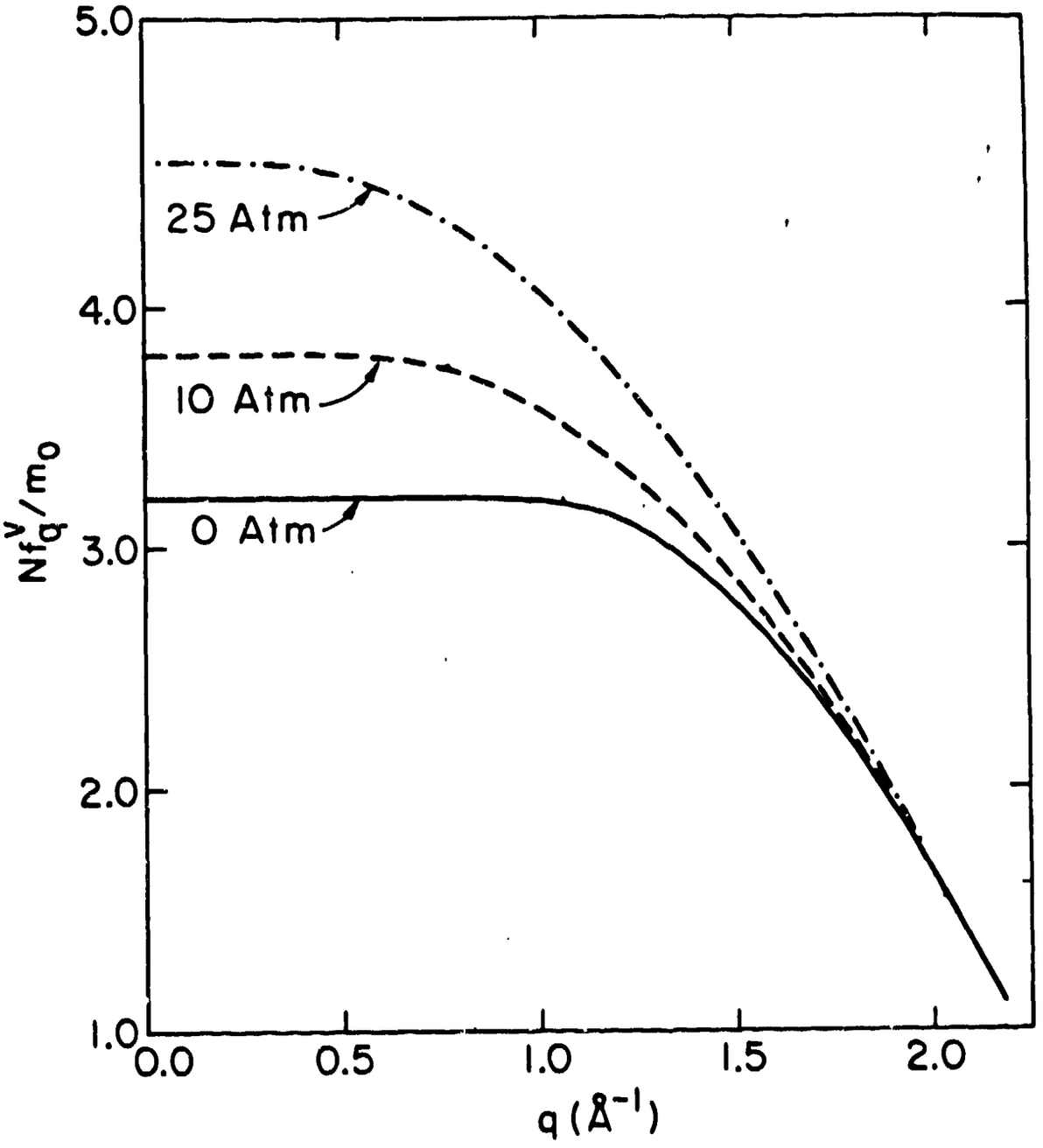


Figure 3

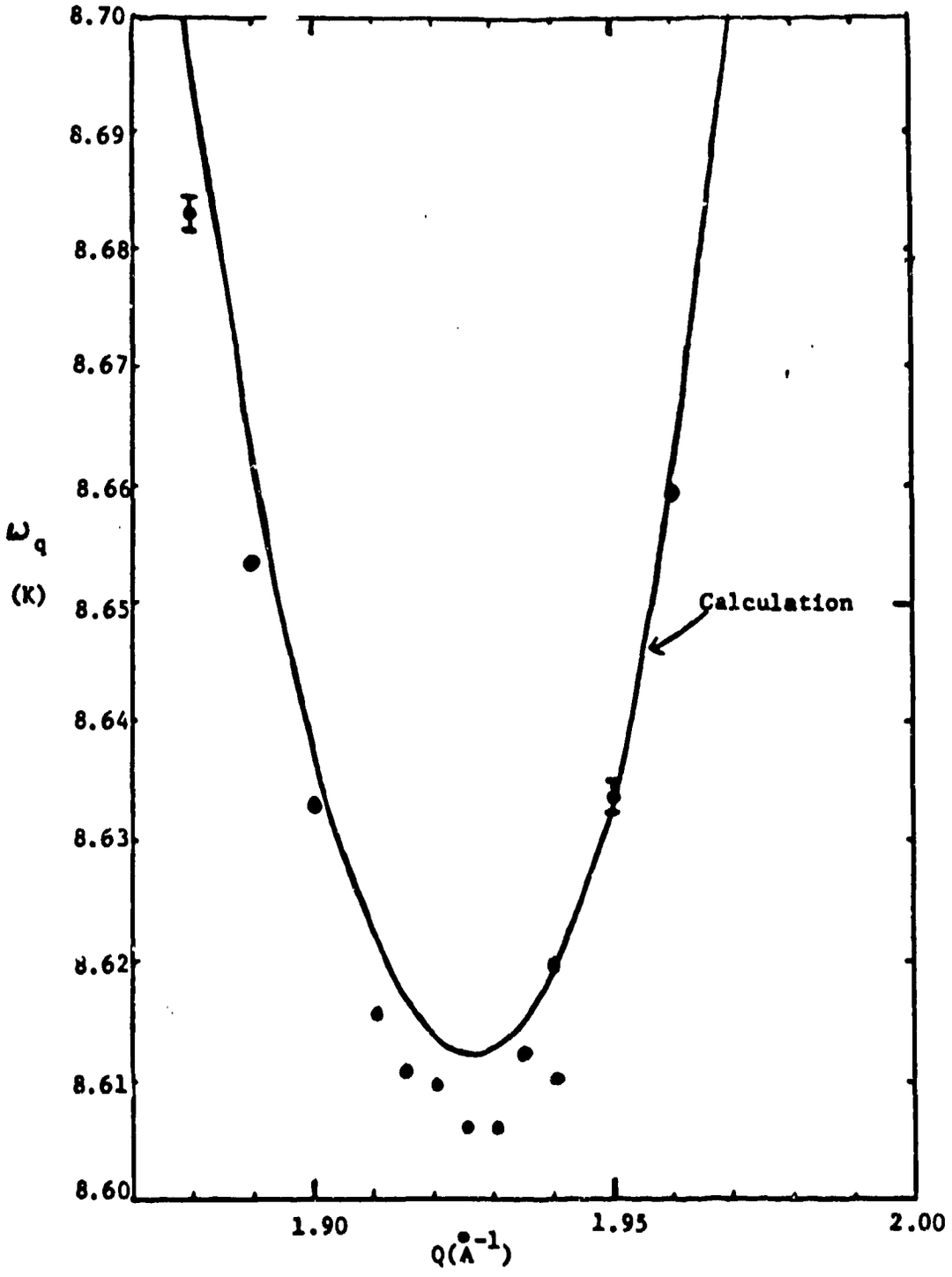
8.70
8.69
8.68
8.67
8.66
8.65
8.64
8.63
8.62
8.61
8.60
$\omega_q$
(K)
Calculation
1.90
1.95
2.00
Q(Å$^{-1}$)

Figure 4

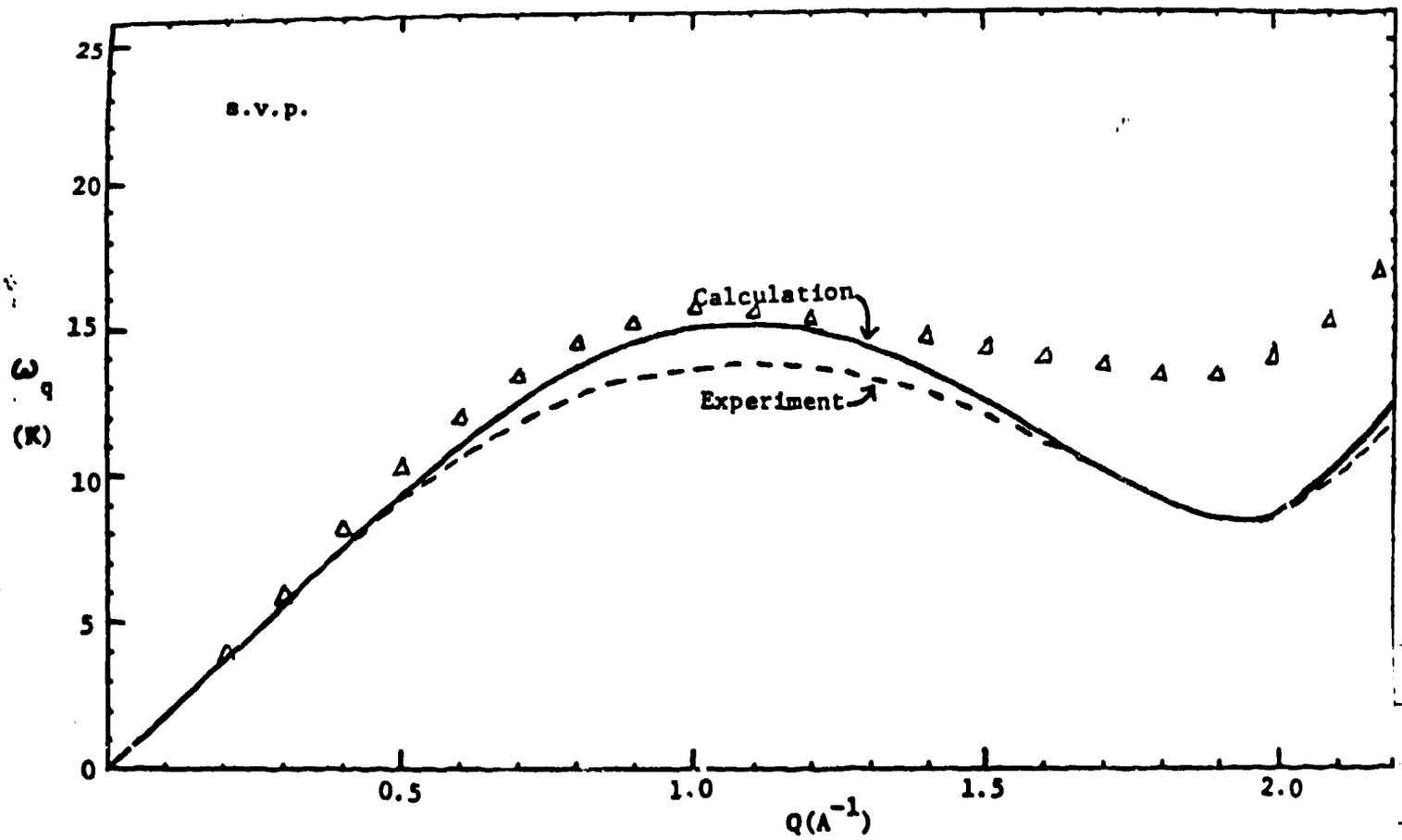
s.v.p.
Calculation
Experiment
$\omega_q$ (K)
25
20
15
10
5
0
0.5
1.0
1.5
2.0
Q(Å$^{-1}$)

Figure 5

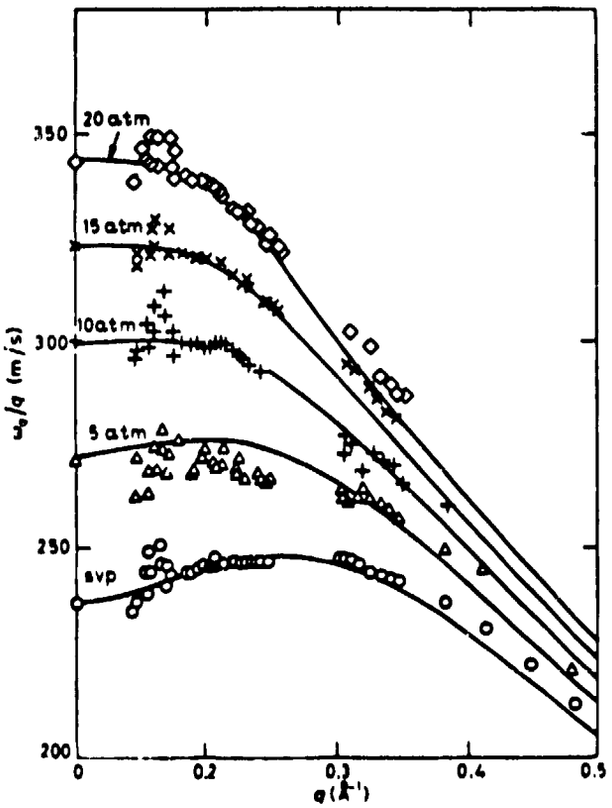
20 atm
15 atm
10 atm
5 atm
svp
350
300
250
200
0
0.2
0.3
0.4
0.5
$\omega_0/q$ (m/s)
$q$ (Å$^{-1}$)

Figure 6

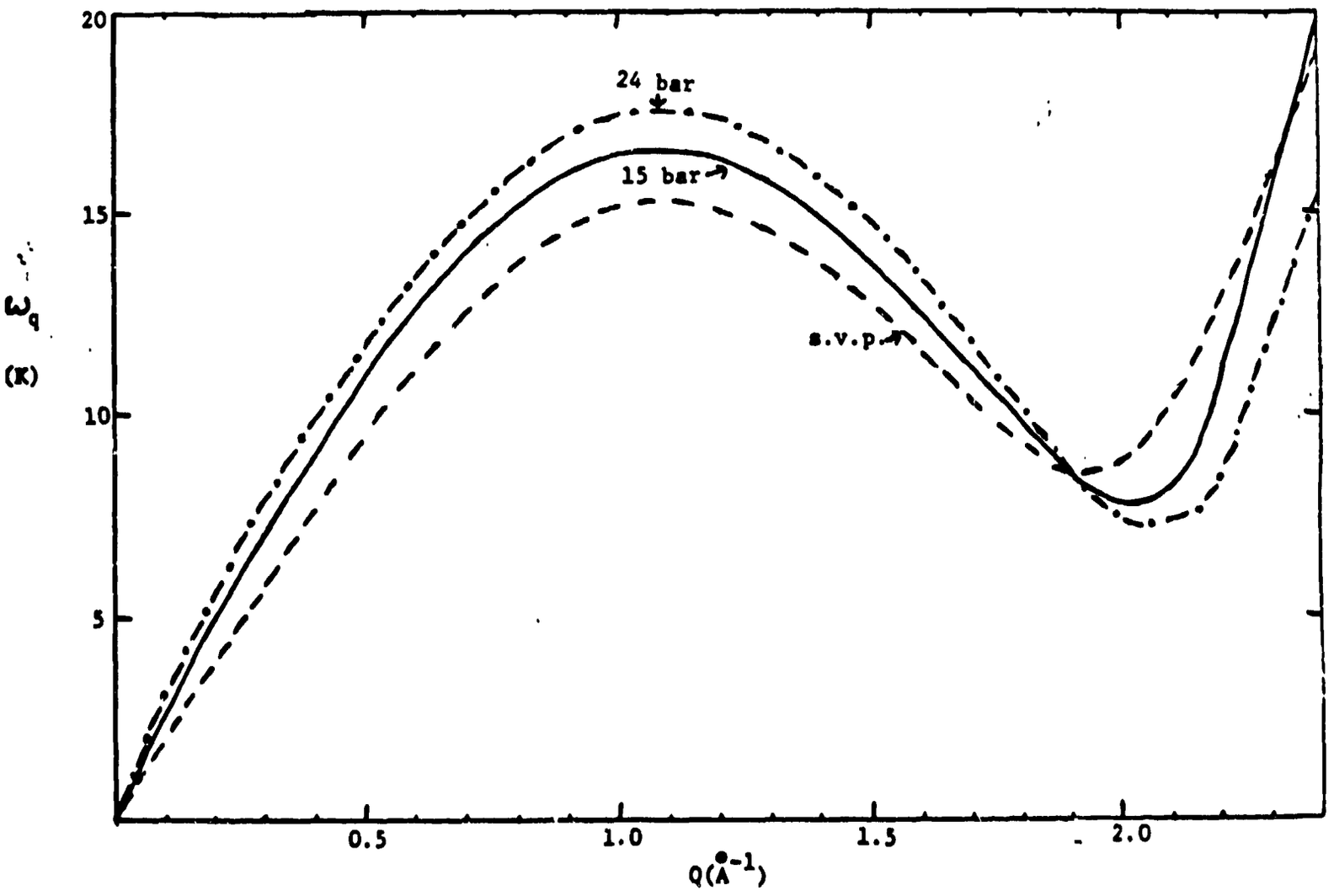


Figure 7

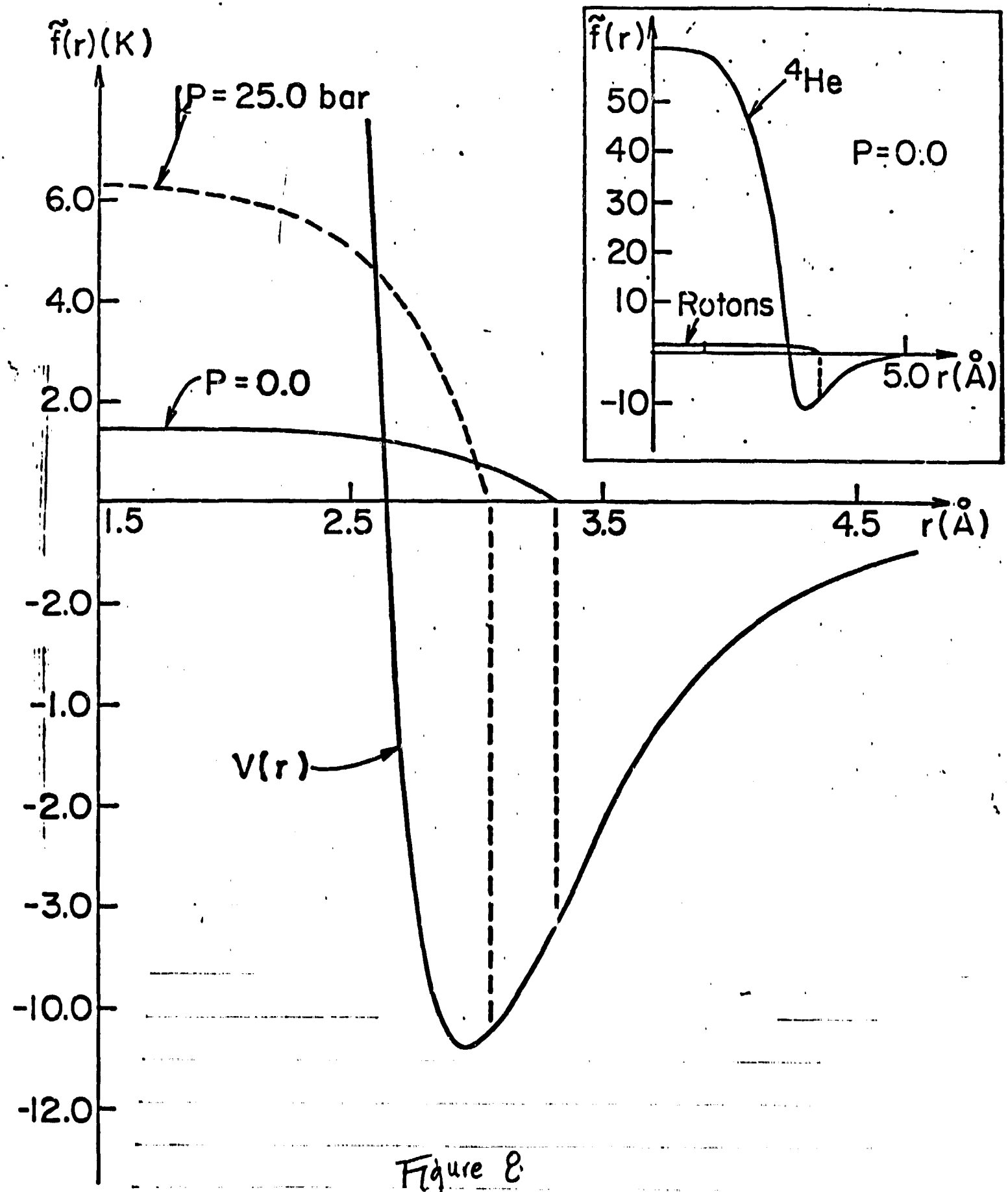
f̃(r)(K)
P = 25.0 bar
6.0
4.0
2.0
P = 0.0
1.5
2.5
3.5
4.5
r(Å)
-2.0
-1.0
-2.0
-3.0
-10.0
-12.0
V(r)
f̃(r)
4He
50
40
30
20
10
Rotons
P=0.0
5.0 r(Å)
-10

Figure 8

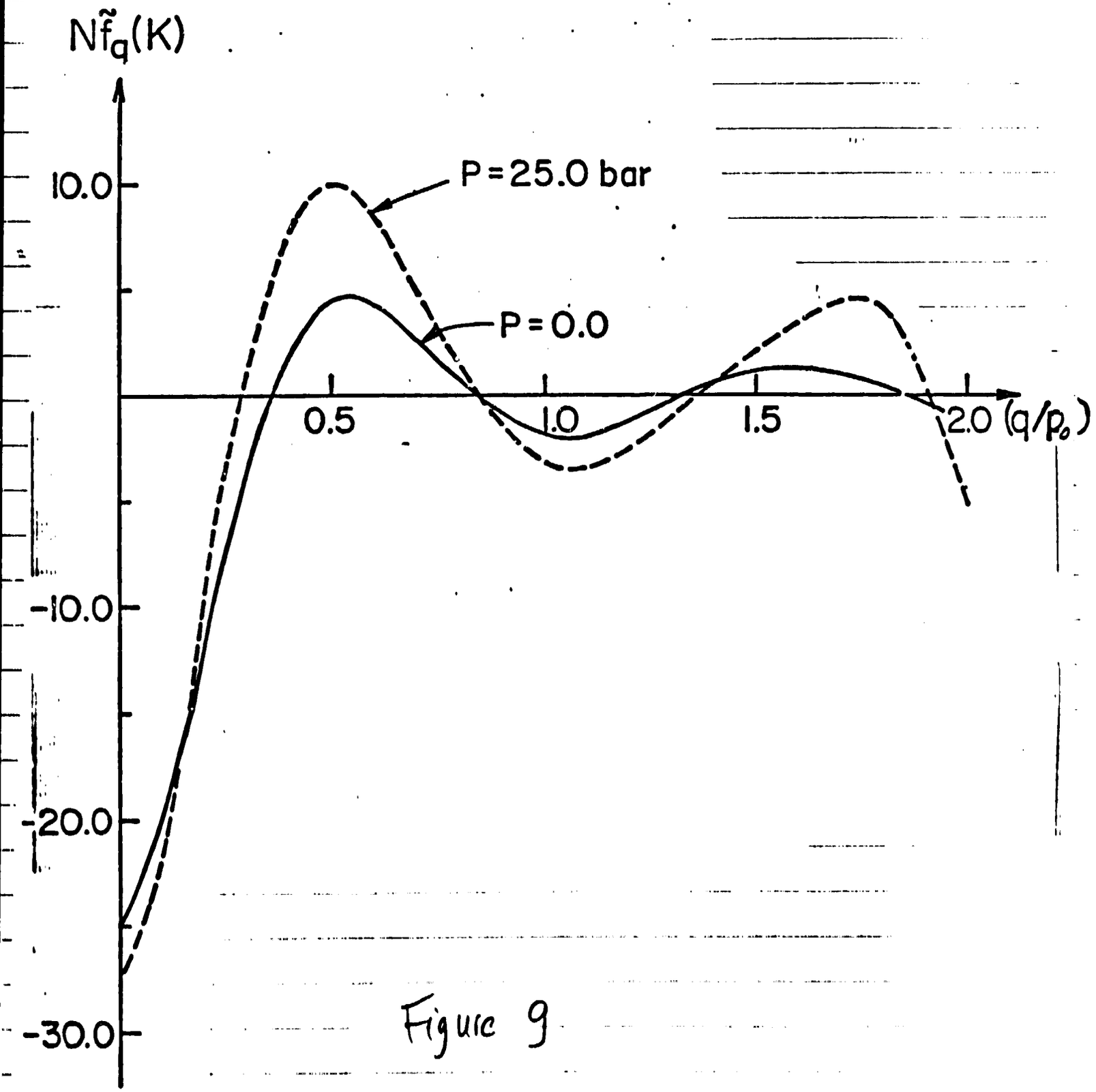


Figure 9

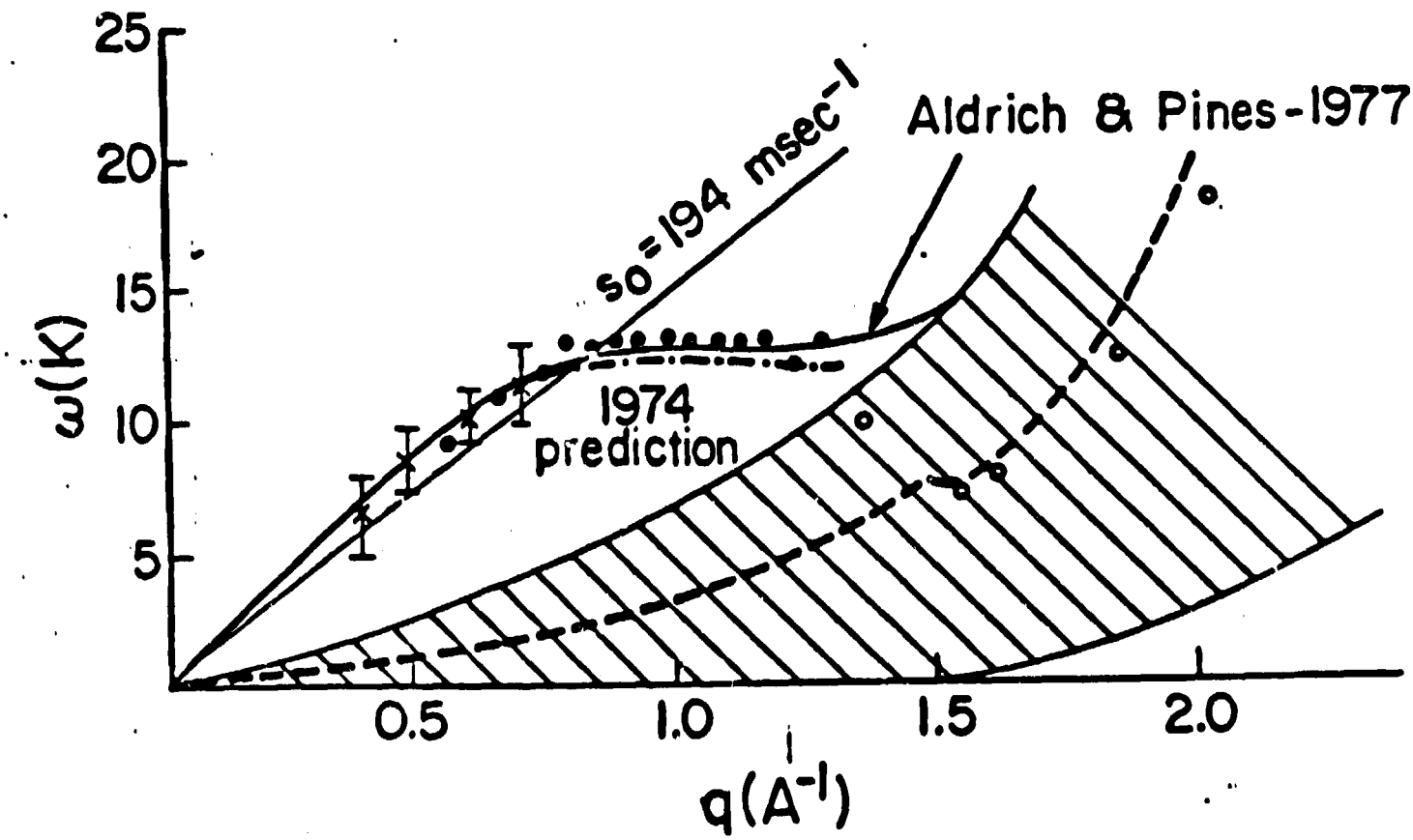
25
20
15
10
5
ω(K)
0.5
1.0
1.5
2.0
q(A⁻¹)
so=194 msec⁻¹
Aldrich & Pines-1977
1974
prediction

Figure 10

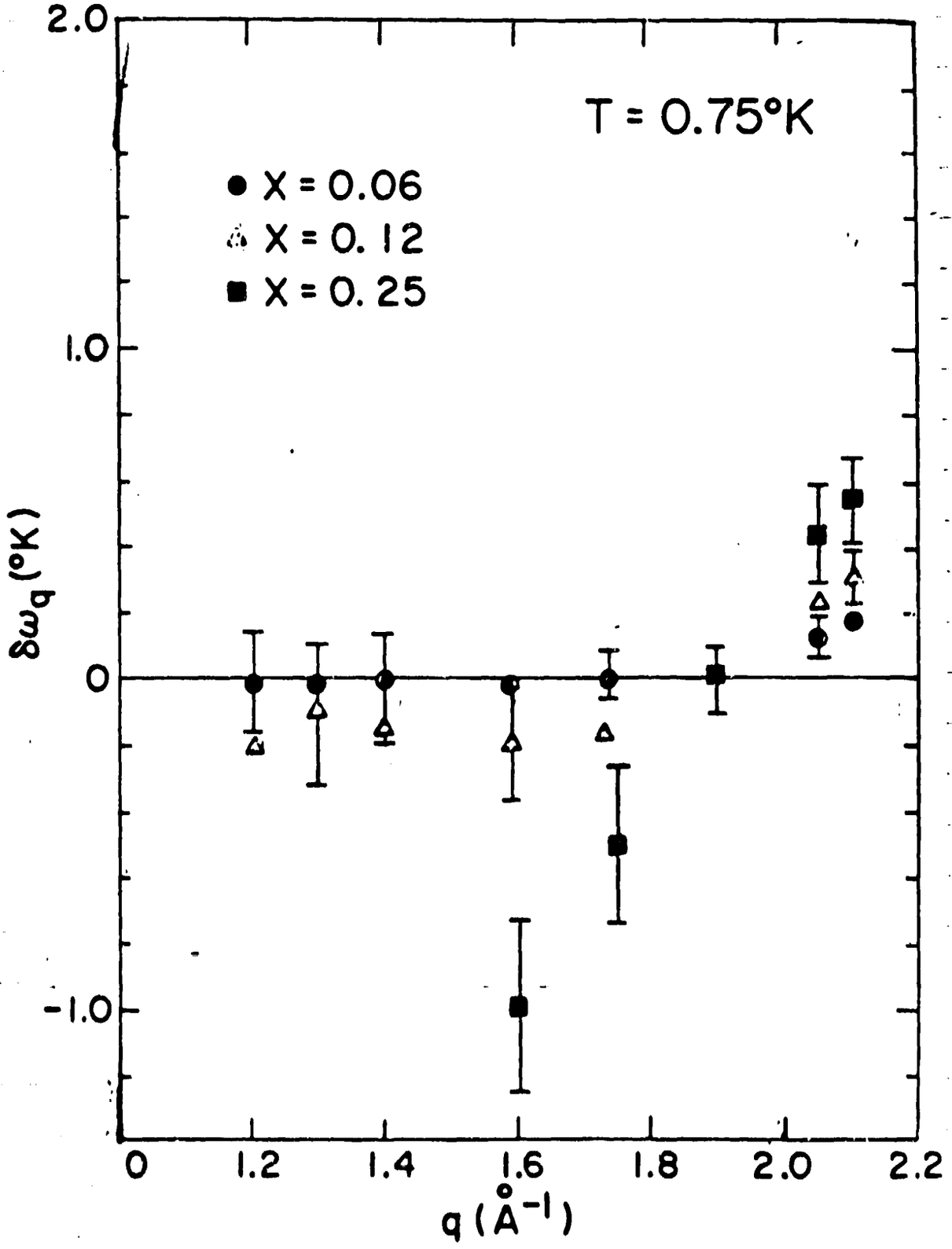
T = 0.75°K
● X = 0.06
△ X = 0.12
■ X = 0.25
2.0
1.0
0
-1.0
$\delta\omega_q$ (°K)
0
1.2
1.4
1.6
1.8
2.0
2.2
q (Å$^{-1}$)

Figure 11

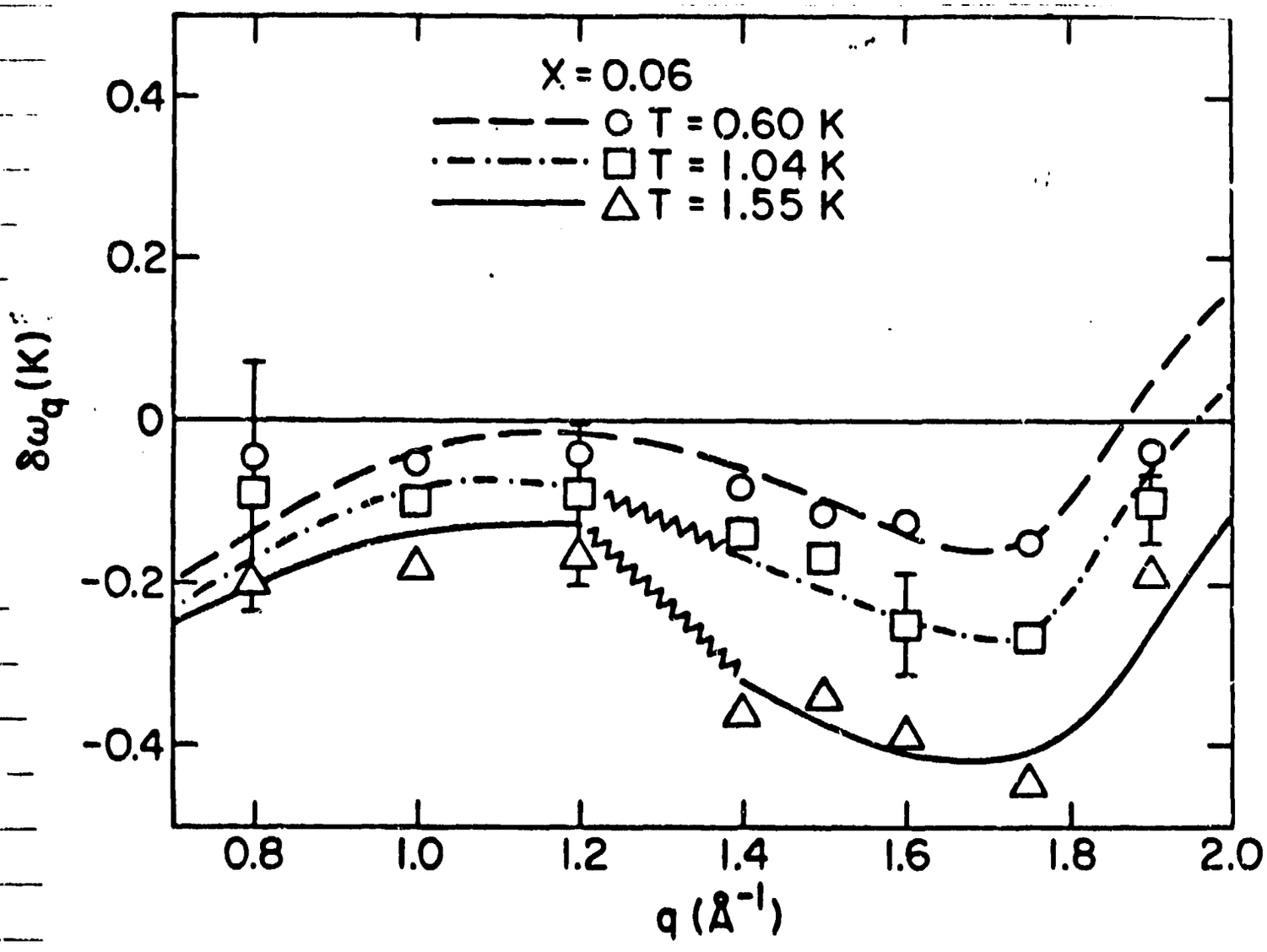
X = 0.06
T = 0.60 K
T = 1.04 K
T = 1.55 K
0.4
0.2
0
-0.2
-0.4
$\delta\omega_q$ (K)
0.8
1.0
1.2
1.4
1.6
1.8
2.0
q (Å$^{-1}$)

Figure 12